

# Analysis of a Heavy Rainfall Event over Beijing During 21–22 July 2012 Based on High Resolution Model Analyses and Forecasts

JIANG Xiaoman<sup>1</sup> (姜晓曼), YUAN Huiling<sup>1,2\*</sup> (袁慧玲), XUE Ming<sup>1,3</sup> (薛明), CHEN Xi<sup>1</sup> (陈曦),  
and TAN Xiaoguang<sup>4</sup> (谭晓光)

<sup>1</sup> School of Atmospheric Sciences and Key Laboratory of Mesoscale Severe Weather/Ministry of Education, Nanjing University, Nanjing 210093, China

<sup>2</sup> Jiangsu Collaborative Innovation Center for Climate Change, Nanjing 210093, China

<sup>3</sup> School of Meteorology and Center for Analysis and Prediction of Storms, University of Oklahoma, Norman 73072, USA

<sup>4</sup> Beijing Institute of Urban Meteorology, China Meteorological Administration, Beijing 100089, China

(Received July 10, 2013; in final form December 25, 2013)

## ABSTRACT

The heaviest rainfall over 61 yr hit Beijing during 21–22 July 2012. Characterized by great rainfall amount and intensity, wide range, and high impact, this record-breaking heavy rainfall caused dozens of deaths and extensive damage. Despite favorable synoptic conditions, operational forecasts underestimated the precipitation amount and were late at predicting the rainfall start time. To gain a better understanding of the performance of mesoscale models, verification of high-resolution forecasts and analyses from the WRF-based BJ-RUCv2.0 model with a horizontal grid spacing of 3 km is carried out. The results show that water vapor is very rich and a quasi-linear precipitation system produces a rather concentrated rain area. Moreover, model forecasts are first verified statistically using Equitable Threat Score (ETS) and BIAS score. The BJ-RUCv2.0 forecasts under-predict the rainfall with southwestward displacement error and time delay of the extreme precipitation. Further quantitative analysis based on the contiguous rain area (CRA) method indicates that major errors for total precipitation ( $> 5 \text{ mm h}^{-1}$ ) are due to inaccurate precipitation location and pattern, while forecast errors for heavy rainfall ( $> 20 \text{ mm h}^{-1}$ ) mainly come from precipitation intensity. Finally, the possible causes for the poor model performance are discussed through diagnosing large-scale circulation and physical parameters (water vapor flux and instability conditions) of the BJ-RUCv2.0 model output.

**Key words:** heavy rainfall, precipitation verification, mesoscale model, rainstorm forecast

**Citation:** Jiang Xiaoman, Yuan Huiling, Xue Ming, et al., 2014: Analysis of a heavy rainfall event over Beijing during 21–22 July 2012 based on high resolution model analyses and forecasts. *J. Meteor. Res.*, **28**(2), 000–000, doi: 10.1007/s13351-014-3139-y.

## 1. Introduction

Heavy rains are commonly responsible for weather disasters in China. Associated with the summer monsoon, three primary rain zones of China in the warm season are located in southern China, Jiang-Huai area, and northern China, respectively (Tao, 1980). In northern China, heavy rains are concentrated in July and August and are mostly caused by strong local con-

vective storms (Compilers of Heavy Rainfall in North China, 1992). Due to complex topography and high population density, heavy rainfall events in this area, especially flash-flood-producing rainfall, can cause significant social and economic losses, and endanger lives.

During 21–22 July 2012, a disastrous rainfall hit Beijing (often referred to as the “7.21” event). Being the heaviest rainfall ever occurred in the last 61 years,

---

Supported by the National (Key) Basic Research and Development (973) Program of China (2013CB430106), China Meteorological Administration Special Public Welfare Research Fund (GYHY201206005), National Natural Science Foundation of China (41175087), and National Fund for Fostering Talents (J1103410).

\*Corresponding author: yuanhl@nju.edu.cn.

it caused widespread havoc in the capital, killing at least 79 people and endangering more than 1.9 million residents. During 0200–2200 UTC 21 July, more than 150-mm rain fell across Beijing. The heaviest precipitation reached 460 mm in Fangshan area, causing catastrophic flood and landslide. This extreme event has caused wide concerns in meteorological community in China. Several studies (e.g., Fang et al., 2012; Sun Jisong et al., 2012) investigated the synoptic and mesoscale conditions and the mechanism of the rainstorm system. Chen et al. (2012) and Sun Jun et al. (2012) discussed the causes of the extreme event, while Yu (2012) analyzed the favorable conditions for this record-breaking rainfall, with the aid of radar observation. Additionally, a number of papers investigated detailed features such as the sources of water vapor, frontogenesis, upper-level jet stream, and so on (Chen et al., 2013; Li et al., 2013; Liao et al., 2013; Quan et al., 2013; Sun et al., 2013). These studies focused on the precipitation dynamics and conditions of this extreme event using various observations, trying to gain a better understanding of its mechanisms. However, discussions on model forecasting performance of this event are rare. In particular, quantitative precipitation forecasts (QPFs) based on high resolution mesoscale models are critical for operational forecasters.

Zhao et al. (2013) showed that the “7.21” event occurred under a typical circulation pattern conducive to heavy rainfall in northern China. The operational models predicted the heavy rainfall amount with skill of various degrees, however, the forecast rainfall start and end times were noticeably delayed (Tao and Zheng, 2013). Though some of the operational models reproduced rainfall accumulation, they did not capture the correct mechanism in the rainfall process (Zhang et al., 2013). Therefore, analysis of the model capability to predict such heavy rainfall is necessary, in order to identify the causes of forecast errors and improve QPF.

In recent years, high performance computing has rapidly advanced the development of numerical weather prediction models on fine scales, with improved physics and data assimilation systems. Veri-

fication is needed to understand the advantages and weaknesses of such model forecasts. However, traditional verification statistics tend to penalize a mislocated precipitation, especially for high resolution mesoscale models, possibly resulting in poor indications of QPF quality using such statistics as Threat Score (TS) and Equitable Threat Score (ETS) (Schaffer, 1990), and BIAS score. As an alternative, Ebert and McBride (2000) developed an objective-oriented verification method within the framework of contiguous rain areas (CRAs). Through this method, the total rainfall error of model forecasts can be decomposed into the components of location, rain volume and pattern, providing quantitative analysis of precipitation errors.

In this work, ETS and BIAS scores are used to provide overall performance of QPF of the mesoscale model forecasts for the “7.21” event, while the CRA method is used to better understand the forecast errors of QPF and model predictability of heavy rainfall. Accordingly, Section 2 describes the data sources (including the BJ-RUCv2.0 model output) and briefly introduces the CRA method. In Section 3, the mesoscale model forecast results are investigated and discussed. Section 4 presents the verification results of precipitation forecasts based on both traditional methods and the CRA method. Section 5 discusses the possible causes of model errors. Finally, the summary and conclusions are given in Section 6.

## 2. Data and method

### 2.1 Data sources

This work is based on various observations and analysis data, which are listed as follows.

- 1) NCEP (National Centers for Environmental Prediction) GFS (The Global Forecast System) 6-h analysis with  $0.5^\circ \times 0.5^\circ$  resolution;

- 2) Hourly merged precipitation product with  $0.1^\circ \times 0.1^\circ$  resolution based on AWS (automatic weather station) observations in China and CMORPH (Climate Prediction Center MORPHing technique) satellite data;

- 3) FY-2E satellite infrared images;

4) Beijing Meteorological Bureau BJ-RUCv2.0 model (Beijing–Rapid Update Cycling data assimilation and forecast system) hourly output data with 3-km resolution (Fan et al., 2013).

The CMORPH merged precipitation data have been developed through the two-step merging algorithm of probability density function and optimal interpolation, which effectively takes the advantages of the AWS observations and satellite product of CMORPH (Shen et al., 2010). Therefore, the merged precipitation product can capture more reasonable precipitation amount and spatial distribution, as well as the mesoscale features of precipitation distribution (Shen et al., 2013). Figure 1 shows the distribution of CMORPH merged precipitation from 0200 to 2200 UTC 21 July 2012. Compared with the observed precipitation released by the Beijing Meteorological Bureau (Sun Jisong et al., 2012), the CMORPH merged data successfully capture the precipitation features and agree well with surface observation. Despite of a weaker rainfall extreme intensity (389 mm) compared to the observed (460 mm), the location of precipitation extreme is accurate. On the other hand, the study area has intensive AWS network with a complete quality control system. In addition, taking into account the good continuity of satellite retrieved data, the

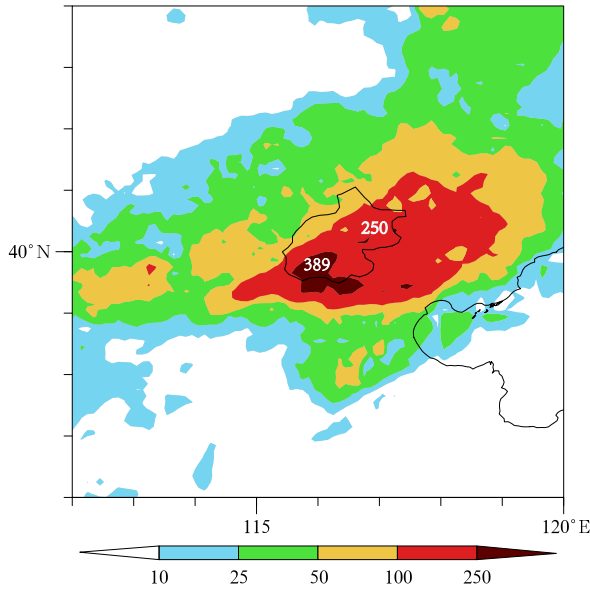


**Fig. 1.** Distribution of CMORPH merged precipitation (mm) from 0200 to 2200 UTC 21 July 2012.

CMORPH merged data have relatively high quality and are therefore used in this work as the observed precipitation for verification.

The BJ-RUCv2.0 is a 3-h update and cycling data assimilation and forecast system based on the WRF (Weather Research and Forecasting) model and WRFDA (WRF Data Assimilation) system (Skamarock et al., 2005). The system contains two domains, with 9- and 3-km grid spacings respectively. The 9-km forecasts are initialized with the cold start at 0000 and 1200 UTC with hourly output. The 3-km forecasts are generated with the cold start initialization at 0000 UTC each day and then run with the diabatic initialization (hot start) every 3 h from 0300 UTC, using the 0–3-h forecasts as the background and the 9-km forecasts as the boundary conditions. Conventional soundings, surface observations, aircraft reports, wind data, the AWS data, and the GPSPW (GPS precipitable water) are assimilated into the system. Based on the BJ-RUC system (Fan et al., 2008; Chen et al., 2010; Lei et al., 2012), the BJ-RUCv2.0 system also assimilates the radar reflectivity and radial velocity of the six Doppler radars in the Beijing-Tianjin-Hebei regions with  $\pm 1$ -h assimilation window through WRF-3DVar (3-dimensional variational system). The effect of assimilating radar reflectivity in the BJ-RUCv2.0 system has been assessed (Fan et al., 2013). In this study, the 3-h analysis data and the 0–24-h forecasts (hourly output) on a 3-km grid of the BJ-RUCv2.0 system are analyzed.

## 2.2 The CRA method

Traditional verification statistics can only provide guidance for the overall performance. For individual event, it is difficult to determine whether the QPF error is brought by the displacement of precipitation or rainfall intensity. This work uses the CRA method (Ebert and McBride, 2000) to verify the QPF of the BJ-RUCv2.0 system, with total error decomposed into the components due to horizontal displacement of the system, error in the mean rain intensity and pattern errors. The CMORPH merged precipitation product is used as the verification data.

The CRA method is carried out following the steps below.

1) Map the forecast and observed fields onto a common grid (in this work, the BJ-RUCv2.0 forecast field is mapped onto the  $0.1^\circ \times 0.1^\circ$  grid). Determine the boundary of CRA by setting precipitation threshold.

2) Shift the forecast field incrementally over the observed field until a “best fit” criterion is optimized. The criterion chosen in this work to determine the best fit is the minimization of TSE (total squared error).

3) Decompose forecast error.

Accordingly, the total mean squared error (MSE) can be decomposed into three components:

$$\text{MSE}_{\text{total}} = \text{MSE}_{\text{displacement}} + \text{MSE}_{\text{volume}} + \text{MSE}_{\text{pattern}}.$$

The total MSE corresponds to the MSE of the original forecast,  $\text{MSE}_{\text{total}} = \frac{1}{N} \sum_{i=1}^N (f_i - o_i)^2$ , where  $f_i$  and  $o_i$  are the forecast and observed rainfall at grid point  $i$ , and  $N$  is the number of gridpoints in the verification domain. After shifting the forecast field, the MSE is recalculated as  $\text{MSE}_{\text{shift}} = \frac{1}{N} \sum_{i=1}^N (f'_i - o_i)^2$ , where  $f'_i$  is the shifted forecast at grid point  $i$ .

The total error due to displacement, volume, and pattern can be then calculated as

$$\begin{aligned} \text{MSE}_{\text{displacement}} &= \text{MSE}_{\text{total}} - \text{MSE}_{\text{shift}}, \\ \text{MSE}_{\text{volume}} &= (\overline{f'} - \bar{o})^2, \\ \text{MSE}_{\text{pattern}} &= \text{MSE}_{\text{shift}} - \text{MSE}_{\text{volume}}. \end{aligned}$$

The overbar denotes the mean value over the domain.

The CRA method can quantitatively determine the attribution of different error components and provide a clearer and more comprehensive insight of the performance of QPF.

### 3. Precipitation features of mesoscale forecasts

As the synoptic circulation provided favorable environment to the “7.21” extreme rainfall, high precipitation efficiency, strong ascending motion, long duration, and extreme abundant water vapor brought together that lead to the heavy rainfall (Sun Jun et al., 2012). Although under the typical circulation condition various operational models predicted the rain

process in advance (e.g., T639 in China, NCEP/GFS, Regional spectral model in Japan), significant errors exist. The GFS 24-h forecast significantly underestimated the precipitation, with the maximum total precipitation intensity lower than 200 mm per 24 h. The 24-h forecast released by the National Meteorological Center of China Meteorological Administration at 2100 UTC 20 July 2012 indicated heavy rainfall in Beijing area with a blue rainstorm warning (over 50 mm per 24 h). However, compared with the observation, the forecast underestimated the precipitation with a southwest displacement error. This work focuses on the real time forecasts produced by the high-resolution BJ-RUCv2.0 system of the Beijing Meteorological Bureau, and evaluates its performance and investigates possible causes of the forecast errors.

The precipitation features of the “7.21” event are firstly reviewed. As shown by the hourly CMORPH merged precipitation distribution (Figs. 2a<sub>1</sub>–a<sub>4</sub>), the precipitation area is quite concentrated with prominent mesoscale feature. The rain starts to intensify at 0600 UTC and gradually increases to reach extreme at 1200 UTC 21 July, presenting a southwest-northeast (SW–NE) oriented mesoscale, quasi-linear rain belt (Fig. 2a<sub>3</sub>). Accordingly, the rainstorm system moves from southwest to northeast, gradually evolves into a convective line, bringing sustained downpour over Beijing. After 1200 UTC, the system heads eastward and moves out of Beijing (Fig. 2a<sub>4</sub>). The corresponding satellite infrared images (figure omitted) also indicate the presence of mesoscale convective complex (MCC). The time series of FY-2E infrared images show that the rain clusters have been developing and maintaining. By 1200 UTC, the black body temperature has decreased to lower than  $-70^\circ\text{C}$ , showing very high cloud top and deep convection. The water vapor channel of satellite images also shows strong SW–NE oriented water vapor transport to the rainstorm center. The embedded MCSs move in a direction consistent with the development of the surface rain belt.

The forecasts and CMORPH merged precipitation are regionally averaged (shown by the red box in Fig. 2a<sub>1</sub>). The time series (Fig. 3) suggest that the forecasts initialized at 2100 UTC 20 July and 0000 UTC 21 July significantly under-predict the observed

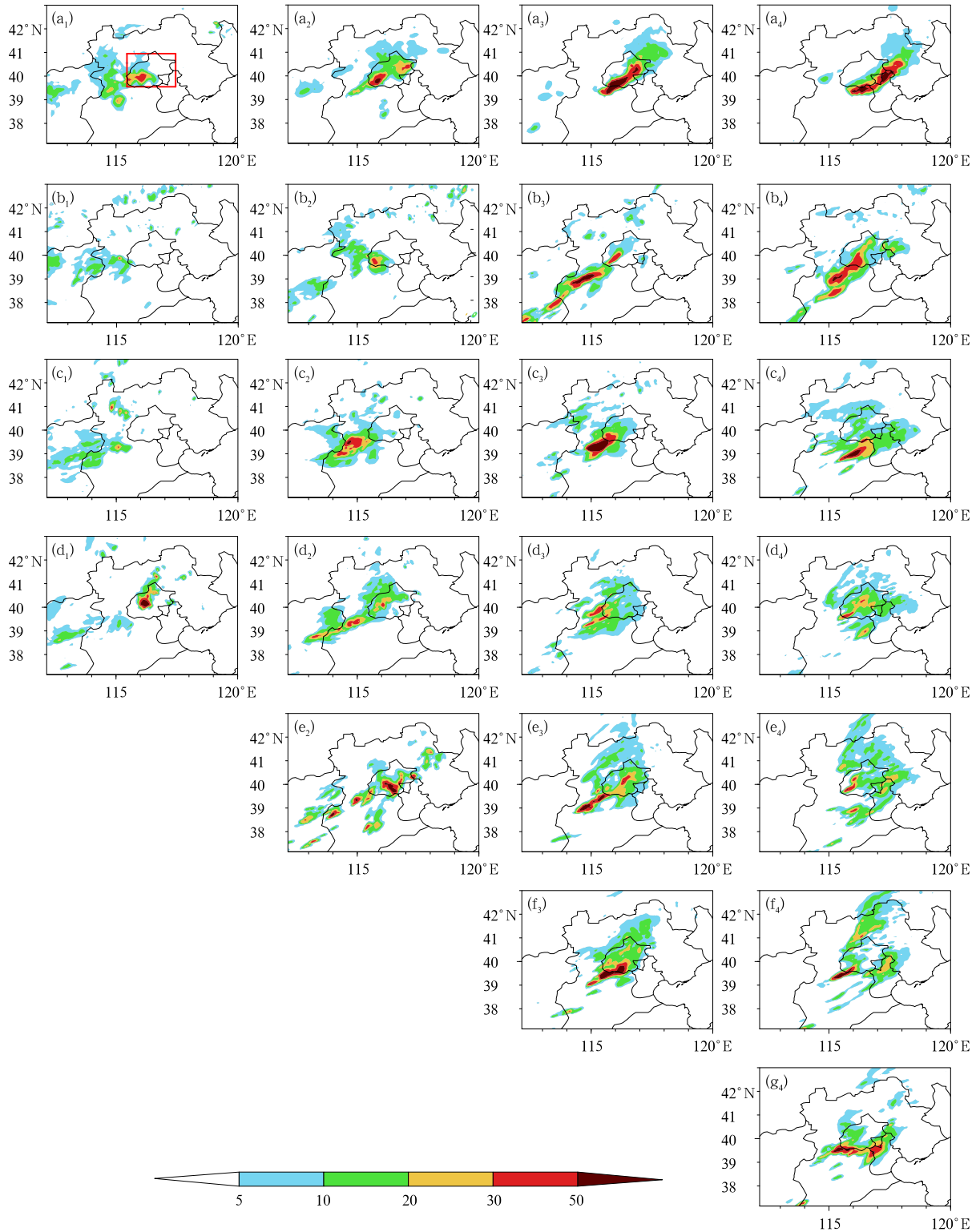


**Fig. 2.** Hourly precipitation (mm h<sup>-1</sup>) at 0600, 0900, 1200, and 1500 UTC 21 July 2012 from (a<sub>1</sub>-a<sub>4</sub>) CMORPH merged precipitation and forecast precipitation initiated at (b<sub>1</sub>-b<sub>4</sub>) 2100 UTC 20 July, (c<sub>1</sub>-c<sub>4</sub>) 0000 UTC, (d<sub>1</sub>-d<sub>4</sub>) 0300 UTC, (e<sub>2</sub>-e<sub>4</sub>) 0600 UTC, (f<sub>3</sub>, f<sub>4</sub>) 0900 UTC, and (g<sub>4</sub>) 1200 UTC 21 July 2012. Valid at (b<sub>1</sub>-d<sub>1</sub>) 0600 UTC, (b<sub>2</sub>-e<sub>2</sub>) 0900 UTC, (b<sub>3</sub>-f<sub>3</sub>) 1200 UTC, and (b<sub>4</sub>-g<sub>4</sub>) 1500 UTC 21 July.

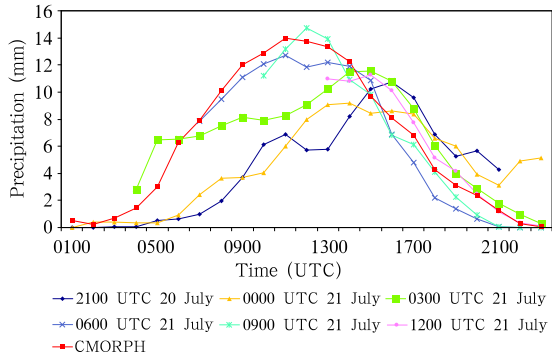


**Fig. 3.** Time series of area averaged CMORPH merged precipitation (mm) and forecast precipitation (mm) at different initial times from BJ-RUCv2.0 output.

precipitation with time delays of 3–4 h, as forecast precipitation peaks at 1500 UTC, compared to the observed peak at around 1200 UTC. The underestimation of regional averaged precipitation is partly due to location displacement (Figs. 2a<sub>2</sub> and 2a<sub>3</sub>), as the forecast rain area falls to the southwest of the observation and thus most rainfall falls out of Beijing area. Precipitation intensity and time series of short-term forecasts (initialized at 0600 and 0900 UTC 21 July) are in a better agreement with the observation. It may result from a better initial field as the BJ-RUCv2.0 system initializes with the cold start at 0000 UTC and assimilates observation data every 3 hours. Therefore, the forecasts initialized after 0600 UTC have already assimilated moisture and hydrometeor information in the initial field, resulting in better forecasts. On the other hand, the cold front passes Beijing at about 1600 UTC (Zhang et al., 2013). Before frontal passage, the precipitation is generated by convective cells along the quasi-linear convective system, while precipitation after 1600 UTC mainly results from frontal rainfall. As indicated by the time series of CMORPH merged precipitation, most of the “7.21” extreme rainfall occurs in the warm sector ahead of the cold front. It is evident that model forecasts underestimate the warm sector precipitation, but predict the front rainfall quite well.

In particular, the forecast initialized at 0300 UTC 21 July is prominently different. The forecast rainfall is rather large at the beginning 3 hours, yet the extreme precipitation is poorly predicted with much lower intensity and significant timing errors. Further

investigation of the precipitation distribution (Figs. 2d<sub>1</sub>–d<sub>4</sub>) shows that data assimilation has a positive impact on the forecast in the initial hours. However, the impact decreases with the forecast hours, leading to the poor forecasts of extreme rainfall.

## 4. Objective verification of QPFs

### 4.1 Statistical scores

Statistical verifications are performed for QPFs from the BJ-RUCv2.0 system. Verification region covers 38°–42°N, 113°–119°E, with 41 × 61 grid-points. The ETSs (Figs. 4a and 4b) verified against CMORPH merged precipitation are generally higher for short-term forecasts, consistent with the subjective evaluation (Figs. 2 and 3). There are large discrepancies in ETSs at the 5 mm h<sup>-1</sup> threshold for different initial times before 1600 UTC 21 July, where short-term forecasts are noticeably superior. After 1600 UTC, the scores are comparable when precipitation is mainly caused by frontal rainfall and the rain gradually decreases (Zhang et al., 2013). In the extreme precipitation period (1100–1400 UTC 21 July), ETSs at 5 mm h<sup>-1</sup> slightly decrease while those at 20 mm h<sup>-1</sup> are relatively high. In addition, it is evident that the scores for short-term forecasts at 20 mm h<sup>-1</sup> reach peak and then decrease quickly at 3 h. Such delayed peak of ETSs may be caused by the adjustment of the model to the 3DVAR analysis. With moisture observations assimilated into the initial field, precipitation forecasts are better with high ETSs at short lead times, and the scores quickly fall with the forecast lead time. Particularly, the ETSs for forecasts initialized at 0300 UTC remain very low at 20 mm h<sup>-1</sup>, in agreement with the earlier discussions.

On the other hand, the BIASs at 5 mm h<sup>-1</sup> (Fig. 4c) indicate forecasts of all initial times over-predict the rainfall to various degrees. In the extreme precipitation period (1100–1400 UTC 21 July), BIASs of all forecasts exceed 1.0. In comparison, the observed frequency decreases in this period, as the precipitation distribution (Fig. 2a<sub>3</sub>) shows a relatively concentrated mesoscale rain belt. The forecasts demonstrate better BIASs for heavy rain (> 20 mm h<sup>-1</sup>) during 1100–1400 UTC, with BIASs of short-term forecasts close

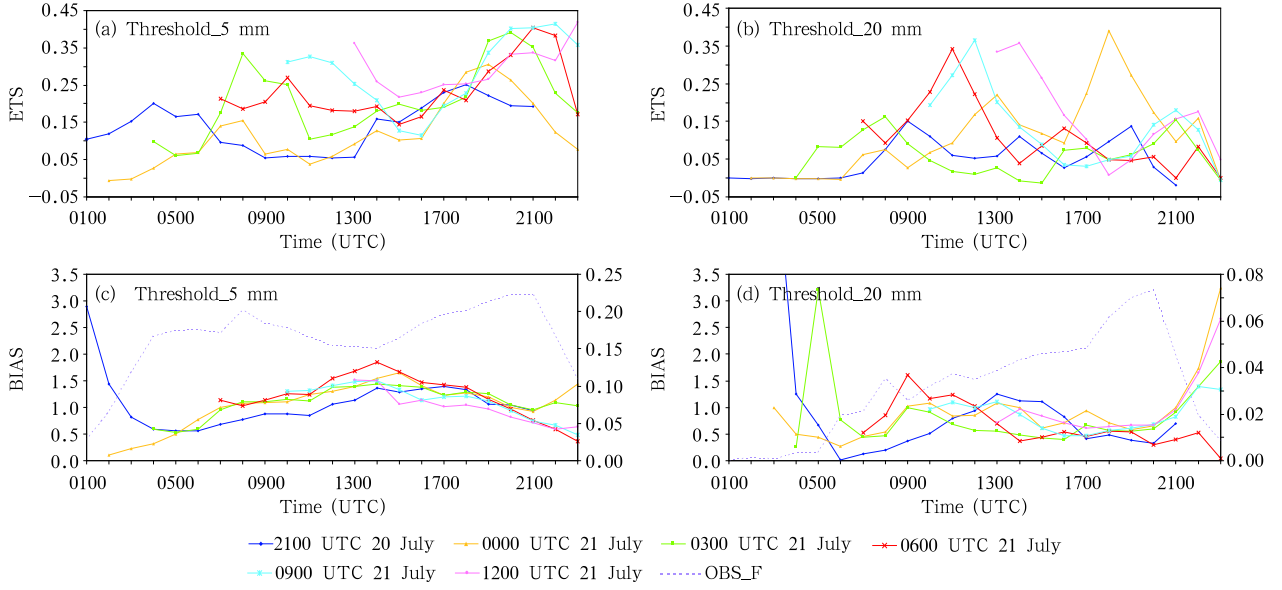


**Fig. 4.** Equitable threat scores (ETS; a, b) and BIAS scores (c, d; observed frequency is indicated by the right ordinate) for different initial times.

to 1.0 (Fig. 4d). The BIASs of forecast initialized at 2100 UTC 20 July are good, while ETSs remain low. Therefore, the forecast number of precipitation grids exceeding the given threshold is comparable to the observation, while the precipitation location and pattern are inaccurate (Figs. 2b<sub>3</sub> and 2b<sub>4</sub>).

#### 4.2 The CRA verification

To compensate for the weaknesses of traditional statistics, the CRA verification is carried out against CMORPH merged precipitation. The forecast rainfall has been interpolated onto the  $0.1^\circ \times 1^\circ$  grid as introduced in Section 2. In general, the model forecasts of different initial times are poorer in the extreme precipitation period (Fig. 5). As for the same validation time, the shorter the lead time, the smaller the root mean square error (RMSE). The model's ability to predict heavy rainfall is eminently poorer with increasing thresholds, as indicated by the much larger RMSE at  $20 \text{ mm h}^{-1}$  than that at  $5 \text{ mm h}^{-1}$ . Moreover, the error decomposition suggests that the majority of total RMSE at  $5 \text{ mm h}^{-1}$  is due to displacement and pattern errors, while the error in forecast mean intensity is quite small. For results at  $20 \text{ mm h}^{-1}$ , the total RMSE mainly results from the volume error. Forecasts from various initial times under-predict the intensity

of heavy rainfall with large precipitation location and shape errors (Fig. 2). For precipitation higher than  $5 \text{ mm h}^{-1}$ , the model predicts a much larger rain area, misrepresenting the observed feature of a linear rain belt and the detailed rain structure.

In addition to the verification of hourly forecasts, the observed and forecast 21-h accumulated precipitation is verified (Fig. 6). Subjective evaluation suggests that the model succeeds in producing a region of extreme rainfall, with the forecast initialized at 0000 UTC 21 July slightly closer to the observations. The forecasts are evidently superior to the GFS forecast, which predicts extreme precipitation lower than  $200 \text{ mm}$  per 21 h. However, the forecast rainfall location falls to the southwest of the observed field. The corresponding CRA verification shows that the total RMSE at  $20 \text{ mm h}^{-1}$  is about  $60 \text{ mm}$ , suggesting rather good results compared with the hourly forecasts. Error decomposition also shows that the majority of the errors, over 50%, is attributable to pattern error, with displacement error accounts for 30%–40% and the mean intensity error nearly negligible.

In conclusion, despite a reasonably good prediction of the accumulated precipitation, more detailed examinations of hourly forecasts show that the real nature of the heavy rain has not been well captured

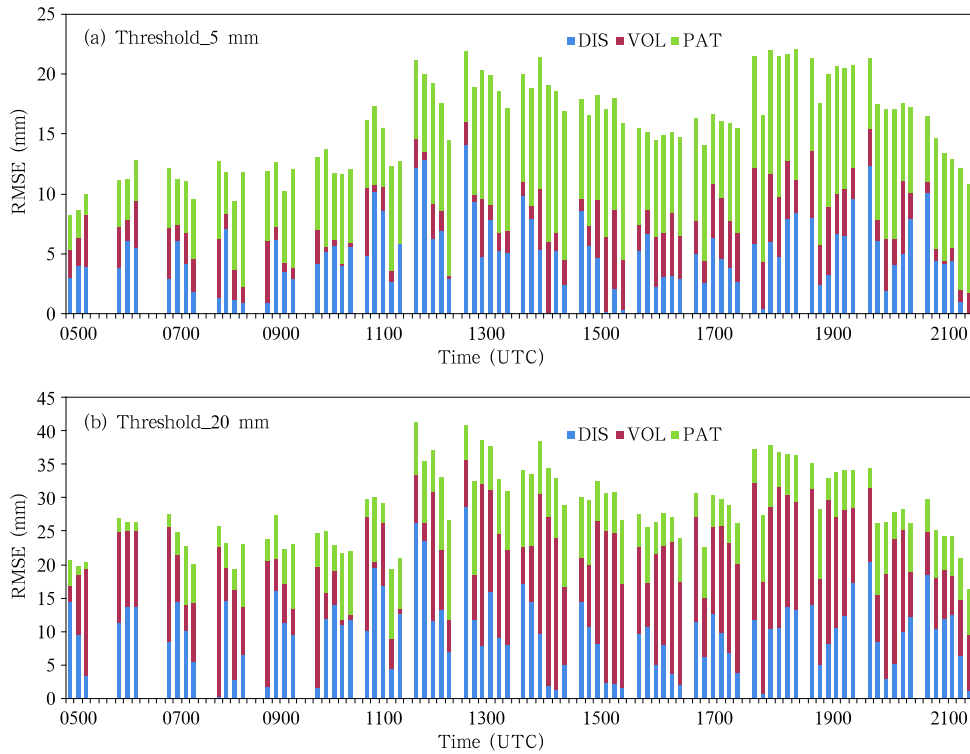


**Fig. 5.** Stacked column charts of the CRA error decomposition. The horizontal axis indicates different forecast valid times, while each column from left to right at each valid time representing forecasts initiated at 2100 UTC 20 July; 0000, 0300, 0600, 0900, and 1200 UTC 21 July 2012.

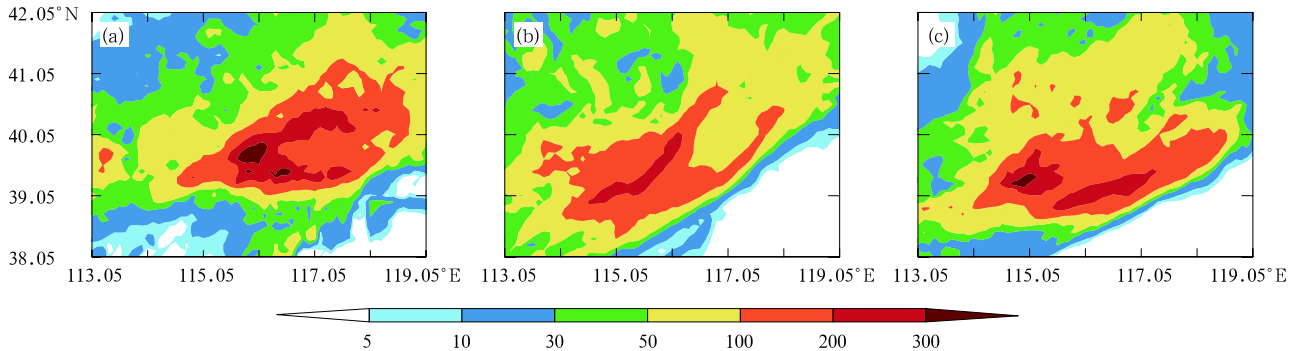


**Fig. 6.** (a) Distribution of CMORPH merged accumulated 21-h precipitation and model forecast precipitation (mm) at initial times (b) 2100 UTC 20 July and (c) 0000 UTC 21 July 2012.

by the model, in other words, the precipitation mechanism is inaccurately represented in the model.

## 5. Diagnosis of the rainfall weather conditions

The above discussion suggests that the model fails to accurately predict heavy rainfall with a large displacement error. To better understand the precipitation mechanism and possible causes of the forecast er-

rors, the synoptic circulation and physical parameters in mesoscale forecasts are diagnosed.

### 5.1 Synoptic circulation

GFS analyses of 500-hPa circulation shows that the eastward moving trough encounters the southwest flow around subtropical high, bringing cold air to intersect with the warm moist flow. Beijing is mainly controlled by the upper southerly winds. For all fore-

cast circulations at different initial times, the trough system in the initial fields quickly disappeared as the model integrates for 2–3 h. At the next analysis time, the observations containing the trough information are assimilated into the initial field; however, the trough is absent once again after model adjustment. In other words, the positive effect of data assimilation only shows at the initial times near the convective development and quickly decreases with the model integra-

tion. The analysis fields consist well with the GFS background circulations, where the short wave systems are absent due to its coarse resolution. Comparing the forecast circulations at different initial times (Fig. 7) with the analysis field (Fig. 7f) valid at 1200 UTC 21 July, each forecast succeeds in predicting the overall circulation of the 500-hPa trough and north-south temperature contrast, as well as the lower 850-hPa winds. However, the short wave trough located over

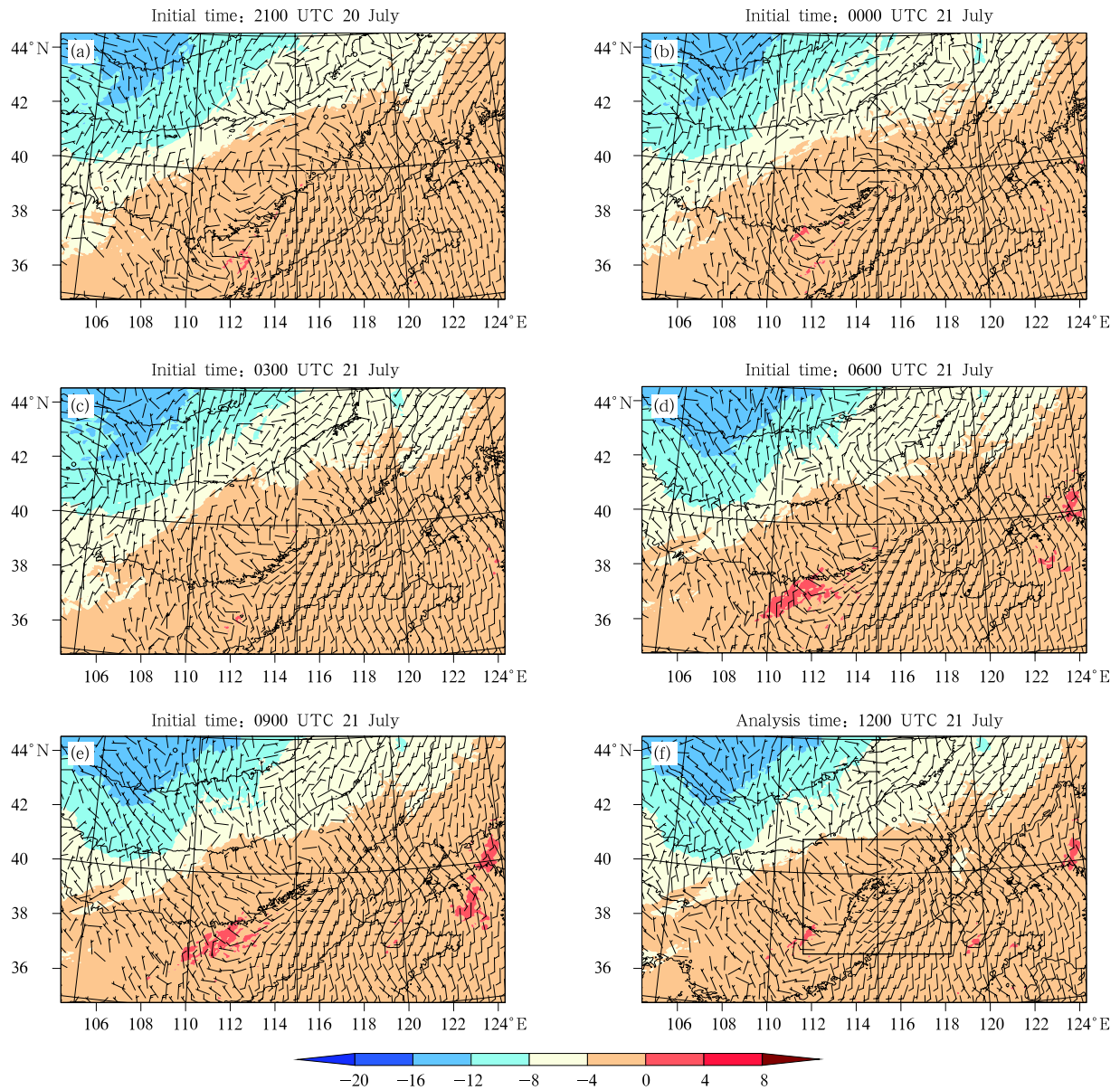


**Fig. 7.** BJ-RUCv2.0 forecasts of 500-hPa temperature (shade; °C), geopotential height (solid line; gpm), and 850-hPa wind (vectors;  $\text{m s}^{-1}$ ) at 1200 UTC 21 July 2012 for initial times (a) 2100 UTC 20, (b) 0000 UTC 21, (c) 0300 UTC 21, (d) 0600 UTC 21, and (e) 0900 UTC 21 July 2012; and (f) analysis field.

Beijing in the analysis field (shown by the red box) is evidently missed in all forecasts. Also, the vortex systems develop slightly to the south in the simulations and affect the precipitation location.

### 5.2 Moisture condition

The evolution of 850-hPa moisture flux indicates a prominent intensification of water vapor transport and its convergence over Beijing from 0600 to 1200 UTC 21 July (figure omitted). The southeast flow and southwest monsoon stream transport water vapor to Beijing continuously, with remarkable water vapor convergence into the rainstorm system. Model forecasts predict well the moisture flux with general intensity and distribution similar to the analyses, representing the southwest and southeast vapor channels. However, the extreme center of moisture flux in the simulations locates a little to the southwest, consistent with the displacement error of the circulation. Accordingly, the distribution of atmospheric precipitable water (PW) shows a favorable moisture condition, as PW exceeds 75 mm by 0600 UTC 21 July (Fig. 8h), also shown in the GFS analysis field (Fig. 8d). The forecast PW (Figs. 8a, 8b, 8e–g) is slightly lower than the analyses (Figs. 8c and 8h). Also, compared with the long and narrow vapor channel extending north on the analysis fields, the high value of PW in the simulations is relatively dispersed with the southward displacement

(Figs. 8a, 8b, 8e–g).

On the other hand, the convergence area of 850-hPa moisture flux corresponds well with the precipitation location. To explore the causes for poor forecasts of rainfall location, the moisture flux convergence is then diagnosed. Analyses show that water vapor divergence turns to convergence over Beijing, with increasing convergence intensity and range. By 0900 UTC 21 July (Fig. 9f), a wide range of strong convergence covers Beijing area, as indicated in the GFS analysis (figure omitted) as well. Meanwhile, the 3-km analysis of the BJ-RUCv2.0 features a southwest-northeast oriented convergence belt, consistent well with the surface rain belt. Short-term forecasts show better performance (Figs. 9d and 9e), while the forecasts initialized before 0600 UTC present a dislocated and dispersed convergence area. In particular, the 0300 UTC run predicts a strong moisture divergence over the rainstorm center, which may lead to poor forecasts with weaker rainfall intensity. Meanwhile, the positive results of forecasts initialized after 0600 UTC exhibit the beneficial effect of the assimilation of more recent observations.

### 5.3 Instability condition

Analysis soundings (figure omitted) calculated from the BJ-RUCv2.0 analyses show that before the rainfall starts, dry intrusion occurs at mid levels,

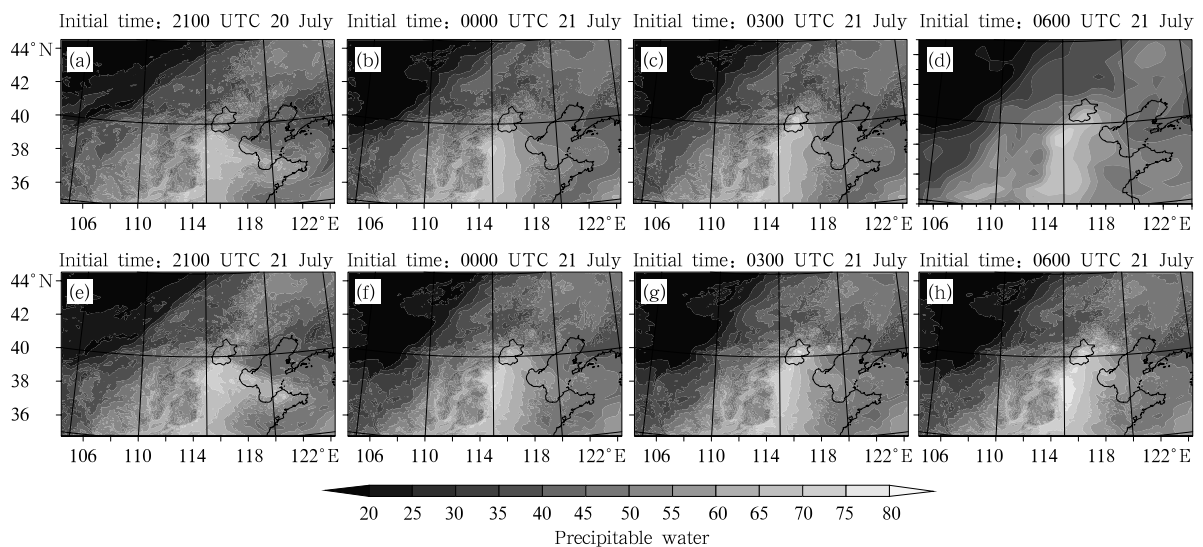


**Fig. 8.** BJ-RUCv2.0 forecasts of precipitable water (shade; mm) for (a, b, e–g) different initial times and (c, h) analysis fields valid at (a–c) 0300 UTC and (e–h) 0600 UTC and (d) GFS analysis field valid at 0600 UTC 21 July 2012.

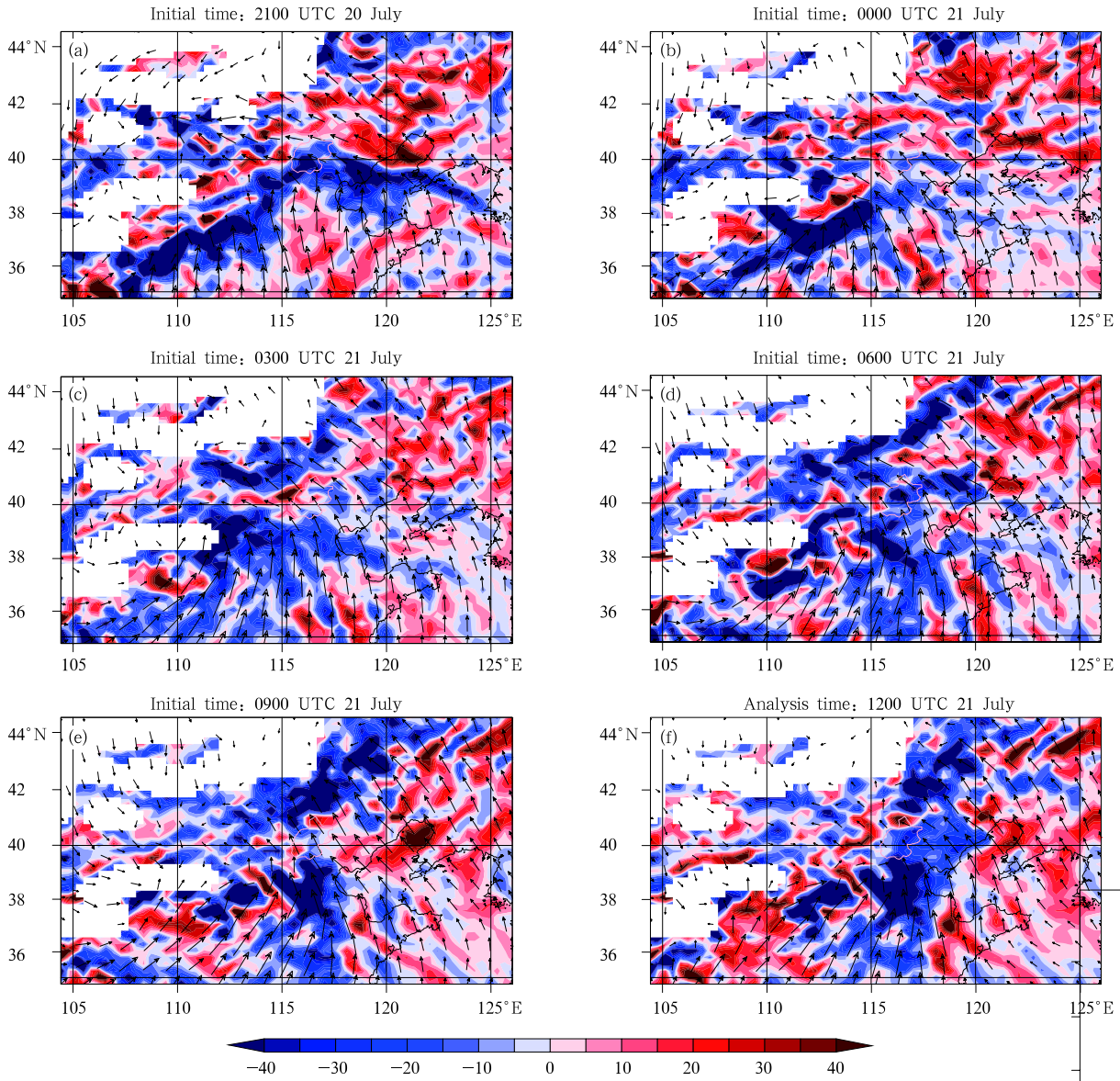


**Fig. 9.** BJ-RUCv2.0 forecasts of 850-hPa moisture flux divergence (shade;  $10^{-5} \text{ g s kg}^{-1} \text{ m}^{-1}$ ) and its corresponding moisture flux (vectors) at 1200 UTC 21 July 2012 for (a–e) different initial times and (f) analysis field.

accompanied by the low-level advection of warm and moist air. By 0300 UTC 21 July, low-level moisture has increased, leading to a rather low lifting condensation level (LCL) and a surge in convective available potential energy (CAPE). Low-level moisture layer over Beijing deepens to almost 10-km thick at 0600 UTC. High value of equivalent potential temperature ( $\theta_e$ ) also extends to lower atmosphere, indicating a favorable condition of moist instability over Beijing. As for the forecasts, the simulated unstable conditions agree

well with the analyses, except for the 0300 UTC run, which shows a small gradient of  $\theta_e$ .

In particular, most of the extreme rainfall occurred in the warm sector ahead of the cold front. Therefore, the movement of the cold front has a rather weak indication of the precipitation. Previous study introduces the concept of “wet baroclinic zone” (usually defined by surface  $\theta_e$ ), which matches well with the precipitation area, especially for the warm sector rainfall (Wang, 2013). Before the rain starts, there ex-

ists a southwest-northeast oriented zone of increasing large  $\theta_e$  gradient, with intensity peaking at 0600 UTC (Fig. 10). The BJ-RUCv2.0 analyses and the AWS observations (Wang, 2013) are highly consistent, indicating rather good quality of the mesoscale model analysis against the GFS analysis (Fig. 10d). Meanwhile, the CAPE reaches  $2000 \text{ J kg}^{-1}$  at this time, suggesting high convective instability. In contrast, the forecasts fail to predict the baroclinic zone. A strong baroclinic zone extending northward is noticeably evident on the analysis fields (Figs. 10c and 10h); however, it is missed by all forecasts. At the same time, the forecast CAPE is much lower than the analyses. As a result, the favorable instability conditions for heavy rainfall are not fully represented in the model simulations. On the other hand, the large  $\theta_e$  gradient region presented at the 0300 UTC analysis (Fig. 10c) is apparently absent in the 3-h forecast (Fig. 10g), indicating again the rapid decrease of the positive effect of data assimilation.

To sum up, the forecasts of different initial times depict the general synoptic scale circulations well, but with southward location errors and the absence of a short wave trough. In terms of physical parameters, moisture peak values are well predicted, reflecting the extremely high water vapor content. However, due to the errors in the system displacement and the mois-

ture convergence, the water vapor has not been correctly concentrated over Beijing area, resulting in the model's poor performance of precipitation location. In addition, despite the positive effect of data assimilation on the initial fields, especially for the times approaching convective development, the beneficial influence decreases with the forecast lead time. The short-wave trough found in the initial analyses generally disappears after 3-h forecasts, affecting subsequent forecast accuracy.

## 6. Summary and conclusions

In this work, using a set of observations and model output, the Beijing "7.21" heavy rainfall case is analyzed, with emphasis on the analysis and verification of 3-km BJ-RUCv2.0 hourly model output. In addition to traditional precipitation verification statistics, the CRA method that is able to separate displacement, volume, and pattern errors is also employed to quantitatively verify the QPFs. In addition, possible causes of inaccurate model forecasts are discussed. The primary findings are as follows:

(1) The heavy rainfall occurred under favorable synoptic conditions with exceptionally abundant water vapor. The precipitation gradually intensified at 0600 UTC and reached its peak at about 1200 UTC

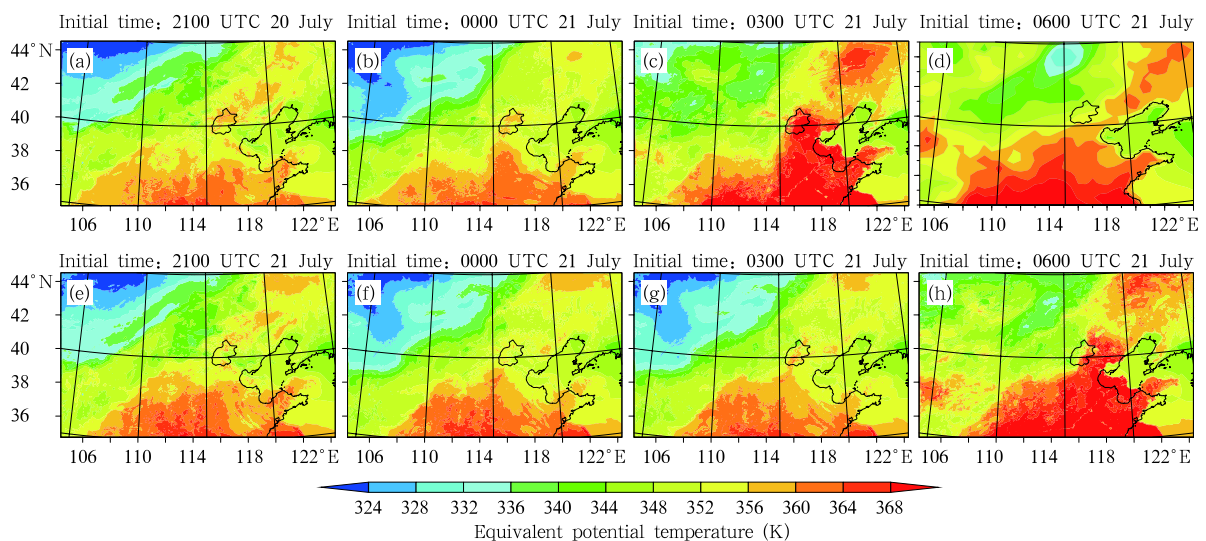


**Fig. 10.** BJ-RUCv2.0 forecasts of surface equivalent temperature (shade; K) for (a, b, e–g) different initial times and (c, h) analysis fields valid at (a–c) 0300 UTC and (e–h) 0600 UTC, and (d) GFS analysis field valid at 0600 UTC 21 July 2012.

21 July 2012. The rainfall area was dominated by a southwest-northeast oriented mesoscale rain belt.

(2) The BJ-RUCv2.0 forecasts under-predicted the observed precipitation with a southwest displacement error and an incorrect representation of the quasi-linear feature of the system. However, short-term simulations obtained higher scores due to the assimilation of moisture and hydrometeor information into the initial conditions. Specifically, the model tends to over-predict light rain ( $> 5 \text{ mm h}^{-1}$ ) while underestimate heavy rainfall ( $> 20 \text{ mm h}^{-1}$ ). Further quantitative error decomposition shows that majority of the total error resulted from the displacement and pattern errors, while the mean intensity error was the major contribution of the error for heavy rainfall ( $> 20 \text{ mm h}^{-1}$ ).

(3) The BJ-RUCv2.0 model forecasts are superior to the GFS forecasts, and the high resolution (3 km) analyses have good quality and are comparable with the observations and the GFS analyses. However, the BJ-RUCv2.0 remains to be further improved for accurately simulating and predicting mesoscale processes. The predicted background circulation is quite similar to the observation, although with a southward displacement and the absence of a short wave trough. Despite the successful simulation of high water vapor, the poor predictions of moisture convergence and instability condition suggest that favorable factors for the heavy rainfall are not fully represented, leading to quite large forecast error. In addition, data assimilation has a positive influence on the initial field, in particular near convection times; however, the positive impact decreases with the model integration. This suggests that the initial analysis fields may not be in a good balance and further improvement to the data assimilation system, especially in the effective use of mesoscale data, is needed.

The Beijing heavy rainfall event, as is the case with many similar cases, involves interactions of weather systems and features at several scales, with complicated processes. Accurate precipitation forecasting is even more challenging due to the quantitative nature and many sources of uncertainties. To improve the accuracy of heavy rainfall prediction, a

better and deeper understanding of the precipitation mechanism is essential. Also, further researches on the data assimilation to optimize initial field and reduce model error are also of practical necessity. This work presents a preliminary analysis on the mesoscale model performance in predicting the Beijing “7.21” extreme rainfall event. However, the results of the BJ-RUCv2.0 system are limited to the specific case and more general conclusions on the predictability of heavy rainfall will require more studies.

**Acknowledgments.** The observation and model data used in this study were provided by the Beijing Institute of Urban Meteorology. The CMORPH merged precipitation data were from the National Meteorological Information Center of China. Dr. Chen Min, Fan Shuiyong, Gao Hua, and other members of the BJ-RUC research group are thanked for their constructive suggestions and help. Professor Tao Zuyu and other reviewers have made review comments that greatly improved the quality of the article.

## REFERENCES

- Chen Min, Fan Shuiyong, Zhong Jiqin, et al., 2010: An experimental study of assimilating the Global Position System—Precipitable water vapor observations into the rapid updated cycle system for the Beijing area. *Acta Meteor. Sinica*, **68**, 450–463. (in Chinese)
- Chen Mingxuan, Wang Yingchun, Xiao Xian, et al., 2013: Numerical simulation study on structure and propagation mechanism of the Beijing extreme heavy rainfall on 21 July 2012 based on radar data 4DVar assimilation. *Acta Meteor. Sinica*, **71**, 569–592. (in Chinese)
- Chen Yun, Sun Jun, Xu Jun, et al., 2012: Analysis and thinking on the extremes of the 21 July 2012 torrential rain in Beijing. Part I: Observation and thinking. *Meteor. Mon.*, **38**, 1255–1266. (in Chinese)
- Compilers of Heavy Rainfall in North China, 1992: *Heavy Rainfall in North China*. China Meteorological Press, Beijing, 1–182. (in Chinese)
- Ebert, E. E., and J. L. McBride, 2000: Verification of precipitation in weather systems: Determination of systematic errors. *J. Hydrol.*, **239**(1–4), 179–202.

- Fan Shuiyong, Guo Yongrun, Chen Min, et al., 2008: Application of WRF 3DVar to a high resolution model over Beijing area. *Plateau Meteor.*, **6**, 1181–1188. (in Chinese)
- , Wang Hongli, Chen Min, et al., 2013: Study of the data assimilation of radar reflectivity with the WRF-3DVar. *Acta Meteor. Sinica*, **71**, 527–537. (in Chinese)
- Fang Chong, Mao Dongyan, Zhang Xiaowen, et al., 2012: Analysis on the mesoscale convective conditions and characteristics of an extreme torrential rain in Beijing on 21 July 2012. *Meteor. Mon.*, **38**, 1278–1287. (in Chinese)
- Lei Lei, Sun Jisong, Wang Guorong, et al., 2012: An experimental study of the summer convective weather categorical probability forecast based on the rapid updated cycle system for the Beijing area (BJ-RUC). *Acta Meteor. Sinica*, **70**, 752–765. (in Chinese)
- Li Na, Ran Lingkun, Zhou Yushu, et al., 2013: Diagnosis of the frontogenesis and slantwise vorticity development caused by the deformation in the Beijing “7.21” torrential rainfall event. *Acta Meteor. Sinica*, **71**, 593–605. (in Chinese)
- Liao Xiaonong, Ni Yunqi, He Na, et al., 2013: Analysis on the key dynamic process in synoptic scale causing extreme moisture environment in “7.21” heavy rain case. *Acta Meteor. Sinica*, **71**, 997–1011. (in Chinese)
- Quan Meilan, Liu Haiwen, Zhu Yuxiang, et al., 2013: The dynamic action of upper-level jet stream in Beijing rainstorm on 21 July 2012. *Acta Meteor. Sinica*, **71**, 1012–1019. (in Chinese)
- Schaffer, J. T., 1990: The critical success index as an indicator of warning skill. *Wea. Forecasting*, **5**, 570–575.
- Shen Yan, Xiong Anyuan, Wang Ying, et al., 2010: Performance of high-resolution satellite precipitation products over China. *J. Geophys. Res.*, **115**, D02114, doi: 10.1029/2009JD012097.
- , Pan Yang, Yu Jingjing, et al., 2013: Quality assessment of hourly merged precipitation product over China. *Trans. Atmos. Sci.*, **36**, 37–46. (in Chinese)
- Skamarock, W. C., J. B. Klemp, J. Dudhia, et al., 2005: A Description of the Advanced Research WRF Version 2. NCAR Tech Note, NCAR/TN-468+STR.
- Sun Jianhua, Zhao Sixiong, Fu Shenming, et al., 2013: Multi-scale characteristics of record heavy rainfall over Beijing area on July 21. *Chinese J. Atmos. Sci.*, **37**, 705–718. (in Chinese)
- Sun Jisong, He Na, Wang Guorong, et al., 2012a: Preliminary analysis on synoptic configuration evolution and mechanism of a torrential rain occurring in Beijing on 21 July 2012. *Torrential Rain and Disasters*, **31**, 218–225. (in Chinese)
- Sun Jun, Chen Yun, Yang Shunan, et al., 2012b: Analysis and thinking on the extremes of the 21 July 2012 torrential rain in Beijing. Part II: Preliminary causation analysis and thinking. *Meteor. Mon.*, **38**, 1267–1277. (in Chinese)
- Tao Shiyun, 1980: *Heavy Rainstorm in China*. Science Press, Beijing, 91–120. (in Chinese)
- Tao Zuyu and Zheng Yongguang, 2013: Forecasting issues of the extreme heavy rain in Beijing on 21 July 2012. *Torrential Rain and Disasters*, **32**, 193–201. (in Chinese)
- Wang Kai, 2013: Isotherm analysis on surface map and cases study on baroclinic zones. Master Dissertation, Sch. of Atmos. Sci., Nanjing University, China, 68 pp. (in Chinese)
- Yu Xiaoding, 2012: Investigation of Beijing extreme flooding event on 21 July 2012. *Meteor. Mon.*, **38**, 1313–1329. (in Chinese)
- Zhang Dalin, Lin Yonghui, Zhao Ping, et al., 2013: The Beijing extreme rainfall of 21 July 2012: “Right results” but for wrong reasons. *Geophys. Res. Lett.*, **40**, 1426–1431.
- Zhao Yangyang, Zhang Qinghong, Du Yu, et al., 2013: Objective analysis of the extreme of circulation patterns during the 21 July 2012 torrential rain event in Beijing. *Acta Meteor. Sinica*, **71**, 817–824. (in Chinese)